Thermal and Magnetic Field Sensors Based on Injection-coupled Devices

V.N. Murashev[1,*], S.A. Legotin[1], P.A. Ivshin[1], K.I. Tapero[2], O.I. Rabinovich[1], D. Elnikov[1],
A.A. Krasnov[1], K.A. Kuz'mina[1]

[1] *National University of Science and Technology "MISIS",*
4, Leninskiy Prospect, 119049 Moscow, Russian Federation
[2] *Research Institute of Scientific Instruments (RISI),*
8, Turayevo, 140080 Lytkarino, Moscow Region, Russian Federation

Operation principle and possible applications of a novel type of silicon integrated circuit (IC) device – injection-coupled device (ICD) – are addressed.

Examples of possible ICD electrical and physical designs are examined in detail. These are based on the existing CMOS and use bipolar technologies.

It is shown that in active mode only one cell of ICD-based sensor chain consumes power. This circumstance enables one to achieve an extraordinarily low power consumption compared to the CMOS ICs. This is because the power consumption of an ICD as a whole is not different of that of a single cell in its IC matrix.

These advantages make ICDs highly attractive for a number of important applications, such as, e.g., radiation detectors or magnetic and thermal field detectors.

Keywords: Sensor, Temperature, Magnetic field, Functionally integrated structure.

PACS number: 85.40. – e

1. INTRODUCTION

There is an obvious incentive for the development of a new generation of electronic sensors, characterized by outstanding performance and wide application area such as simultaneous thermal and magnetic field measurement.

Accordingly, the possible applications of a novel type of silicon cell integrated circuits–injection-coupled devices (ICD) [1-3] as a thermal and magnetic field sensors–is addressed in this paper.

2. OPERATION PRINCIPLE OF ICD

The schematic diagram of ICD is a chain of similar serial-connected cells of a solid silicon integrated circuit as shown in Fig. 1.
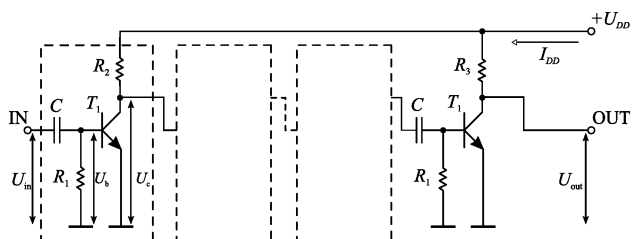

Fig. 1 – Schematic diagram of ICD

The output of each cell is connected to the input of the subsequent cell. Each cell contains a bipolar transistor T_1, capacitor C, base resistor R_1 and collector resistor R_2 (each single cell is shown by a dashed line).

The circuit operates as following. If a negative (or positive) long electric pulse V in is applied to the input of the first cell, the R1C chain differentiates this signal. The fall time constant for the negative pulse τc is equal to the rise time constant for the positive pulse and can be defined as

$$\tau_c = R_1 \cdot C, \qquad (1)$$

where τ_c is the fall time constant, R_1 is the resistance of the base resistor, C is the resistance of the base capacitor.

As a result, two short pulses reach the base of the transistor T_1 (Fig. 2). The short positive pulse is powerful enough for opening the transistor and putting it in a saturation mode. The time τ_{sat}, during which the transistor is saturated, depends on the relationship between resistors R_2 and R_1, transistor gain h_{21E} and the life time of the minority carriers in the base region of the transistor τ_0:

$$\tau_{sat} \approx \tau_0 \cdot \ln (h_{21E} \cdot R_2 / R_1) \qquad (2)$$

where τ_{sat} is the saturation time, τ_0 is the life time of the minority carriers, h_{21E} is transistor gain, R_2 is the resistance of the collector resistor, R_1 is the resistance of the base resistor.

The output signal from the collector of the transistor is applied to the input of the next cell, and the process is repeated again there. So, the pulse applied to the input of the first cell will propagate sequentially through the full chain of cells with the delay equal to τ_{sat} in each cell. The signal propagation time (the time of the cycle T_c) through the full chain from the first to the last cell can be obtained using the equation

$$T_c = n \cdot \tau_{sat} \qquad (3)$$

where T_c is the time of the cycle, n is the number of cells, τ_{sat} is the saturation time.

Single pulse on input of ICD cause the voltage pulses in the power supply circuit. The pulse count is proportionally with the life time of the minority carriers e. g. with influence quantity. The number of pulses arriving with given time interval T_c is logged by the counter.
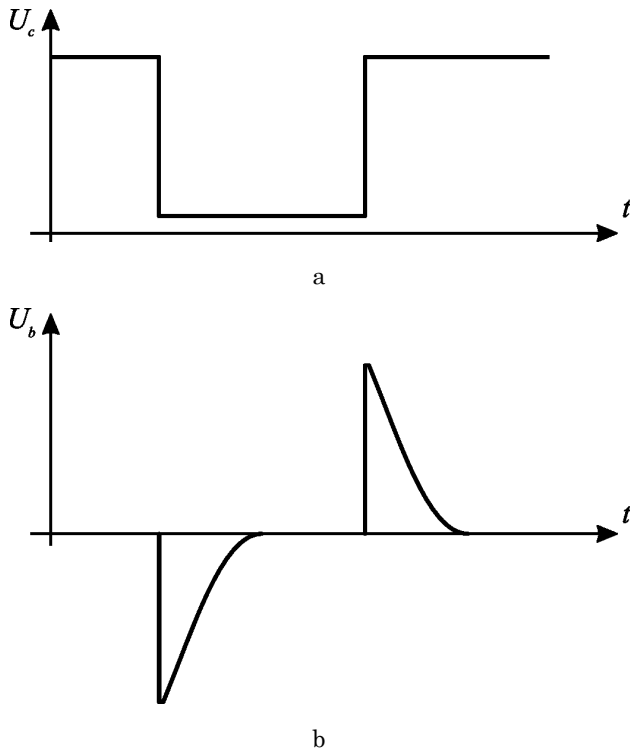
---

* vnmurashev@mail.ru

Fig. 2 – Pulse waveform at the input of a cell (a), at the base of the transistor T_1 (b)

The most important ICD features are:

– extraordinarily low power consumption, because at normal operating conditions only one cell, being in an active operating mode, consumes power (if one neglects leakage currents in the transistors);

– high reliability due to, sort of, a redundancy that is achieved by designing the ICD as a duplicated spiral coil;

– the accuracy of measurement of the external influence (temperature, magnetic field etc.) depends linearly on the number of cells in a ICD chain (3). This number can be very high in integrated circuits. In this case, the technological parameter spread for elements of cells (resistors, capacitors) and fluctuation in minority carrier life time in transistors will hardly affect the results of measurements.

This circumstance, in addition to high reliability and low power consumption, enables one to create high-precision sensors for measurements of temperature field on various surfaces and for localized measurements of the environment temperature. Sensors can be employed in various integrated circuits depending on the application. A variety of technologies (bipolar or MOS) can be used for this purpose.

Various types of ICD based sensors are described below.

3. ICD APPLICATIONS

3.1 Temperature Sensor

The equations (2) and (3) indicate that the saturation time τ_{sat} and the time of the cycle T_c depend linearly on the minority carrier life time τ_0. In silicon, τ_0 is defined by the location of Fermi level with respect to the levels

for recombination centers in the band-gap. The location of Fermi level is known to depend on the dopant concentration and temperature, so that the minority carrier life time is temperature dependent (Fig. 3).
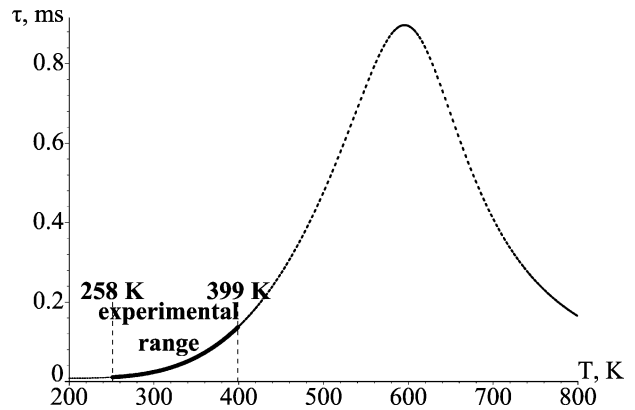

Fig. 3 – Minority carrier life time for n-type semiconductor vs. temperature

So, there is a capability of determining the temperature by measuring the time T_c of the cycle.

An example of a design of a cell fabricated using the standard bipolar isoplanar technology is shown in Fig. 4. The cell contains a vertical bipolar *n-p-n*-transistor, polysilicon base (R_1) and collector (R_2) resistors and a capacitor based on a *p-n*-junction.
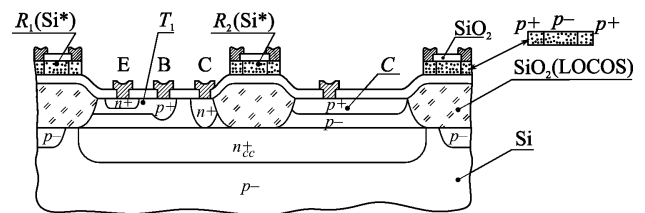

Fig. 4 – Cell design for ICD based temperature sensor with vertical *n-p-n*-transistor

3.2 Magnetic Field Sensor

Fig. 5 presents the cell design for magnetic field sensor. The main difference of this structure from the described above is that this cell uses the capacitor based on MOS structure. Moreover, the base region is isolated by *p-n*-junction and has a greater extent in one of lateral directions. It provides higher magnetic declination of electrons and an increase in their path length in the presence of magnetic field [2] that increases substantially the cell delay time.
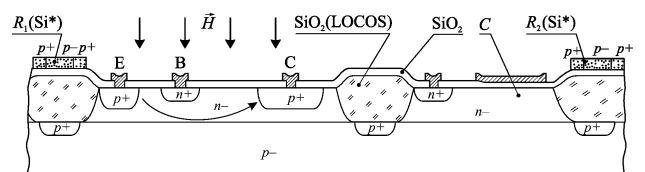

Fig. 5 – Cell design for ICD based magnetic field sensor

4. EXPERIMENT AND ITS RESULTS

To study the functionality of an ICD based temperature sensor a special test bench comprised of 200 cells was made [8, 9] (Fig. 6).

Each cell contained:

− a silicon bipolar *n-p-n*-transistor BC847 with the cutoff frequency of 100 MHz, the gain of not less than 90, collector-emitter breakdown voltage of 45 V, the capacitance of the collector and the emitter *p-n*-junctions of 1.5 and 11 pF, respectively;

− two 0805 type surface-mounted 10 and 200 k□ resistors;

− a 0805 type surface mounted 20 pF capacitor.

The temperature was measured using the model of ICD based sensor and also using the reference digital thermometer DS1624 (Maxim). The measurement was performed in the range of 258-297 K within a cold chamber and in the range of 297-399 K within a thermostat. The time T_c of cycle was measured as a function of temperature. This time was determined by the number of clocks per cycle. Fig. 7 shows the results of the measurements. Each experimental point in this figure was obtained using four measurements. The standard deviation is shown as well.
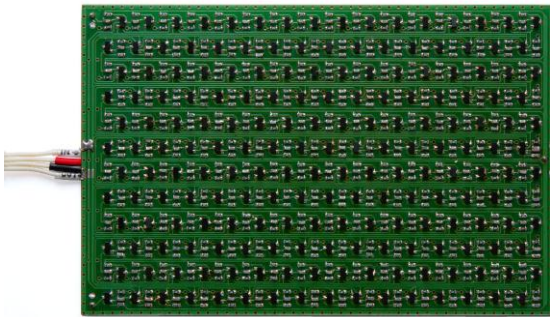

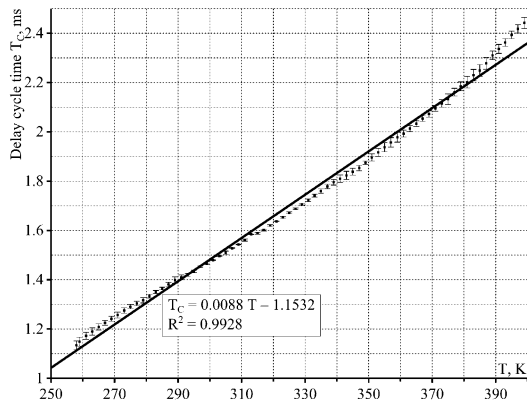**Fig. 6** – The photo of ICD based temperature sensor model

Fig. 7 – Dependence of delay time (time of a cycle) on temperature

As evident from the figure, an increase in temperature of 1 K leads to the increase in the delay time of 10 μs that corresponds to 100 pulses of quartz oscillator. The accuracy of measurement of temperature is higher than 0.01 K. It can be also expected that the parameters spread and the noise level for different elements of sensor chain will not affect significantly the results of the measurement. The delay time T_c (the time of one cycle) and the accuracy of the measurement depend linearly on the number of cells in the ICD based sensor chain.

5. CONCLUSIONS

ICDs can be considered as promising devices for the new generation of sensors. ICDs are characterized by high reliability, low power consumption, simple fabrication technologies, effective digital output signals and a possibility of integration of different types of sensors in one chip. These features can be considered as crucial advantages of ICDs in comparison with the existing sensor types.

The usage of ICDs in sensor systems on flat surfaces can be considered as the most promising one. Such systems can be applied for

− investigation of distribution of temperature on human body surface in medical applications;

− measurement of distribution of temperature on crystal surfaces;

− thermal sensor units in automatic fire-extinguishing systems etc.

Also ICDs could be used as cells of position-sensitive radiation detectors [10, 11].

An example of single IC implemented ICD-based temperature sensor is shown on Fig. 8. The IC include the ICD as a sensor of its own, the counting unit (a counter and a count pulse oscillator) and the serial interface unit interchanging digital data with the microprocessor.
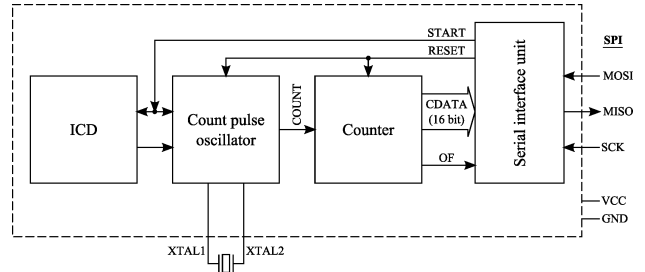

Fig. 8 – An example of the ICD-based IC implementation

In this example the count pulse oscillator has the quartz crystal control.

The serial interface unit has two data lines MOSI and MISO and a clock line SCK (SPI interface). This unit initiate the device reset and measurement start on command from the microprocessor. Upon completing the measurement the pulse count from the counter (CDATA), overflow flag (OF) and other status data (not shown here) load into the serial interface unit registers. All received data transfer to the microprocessor.

AKNOWLEDGEMENTS

REFERENCES

1. V.N. Murashev, Pat. 2147772, Russian Federation, publ. 20.04.2000.
2. V.N. Murashev, S.A. Legotin, Pat. 2392672, Russian Federation, publ. 20.07.2009.
3. V.N. Mourachev, Pat. WO/2006/132560, WIPO, G11C 11/401 (2006.01), G11C 19/00 (2006.01), publ. 14.12.2006.
4. V.V. Gorbachev, L.G. Spitsyna, *Physics of Semiconductors and Metals* (Moscow: Metallurgy: 1982) [in Russian].
5. H. Blanchard, F. de Montmollin, J. Hubin, R.S. Popovic, *Sensor. Actuat. A: Phys.* **82** No 1-3, 144 (2000).
6. V.N. Mordkovich, M.L. Baranochnikov, A.V. Leonov, A.D. Mokrushin, H.M. Omelyanovskaya, D.M. Pazhin, *Sensor. Systems* No7, 33 (2003).
7. T. Saito, V.N. Murashev, A.I. Manyushin, E.F. Karpov, V.N. Mordkovich, E.S. Gornev, G.Ya. Krasnikov, Pat. 2196981, Russian Federation, publ. 20.01.2003.
8. S.A. Legotin, P.A. Ivshin, V.N. Murashev, M.N. Orlova, A.V. Sotnikov, *Proc. Universities. Series: Mater. Electron. Technics* No 4, 63 (2007).
9. S.A. Legotin, P.A. Ivshin, A.S. Korol'chenko, V.N. Murashev, *Instrum. Exp. Tech* **53** No 6, 788 (2010).
10. V.N. Murashev, S.A. Legotin, O.M. Orlov, A.S. Korol'chenko, P.A. Ivshin, *Instrum. Exp. Tech* **53** No. 5, 657 (2010).
11. D.L. Volkov, D.E. Karmanov, V.N. Murashev, S.A. Legotin, R.A. Mukhamedshin, A.P. Chubenko, *Instrum. Exp. Tech* **52** No. 5, 655 (2009).